Available online at www.sciencedirect.com
SCIENCE DIRECT®
Thermochimica Acta 419 (2004) 215–221
thermochimica acta
www.elsevier.com/locate/tca

Thermogravimetric study of the sulfurization of $SrTiO_3$ nanoparticles using CS_2

Jhon Cuya, Nobuaki Sato*, Katsutoshi Yamamoto, Hideyuki Takahashi, Atsushi Muramatsu

Institute of Multidisciplinary Research for Advanced Materials, Tohoku University, 2-1-1 Katahira, Aoba-ku, Sendai 980-8577, Japan

Received 13 November 2003; received in revised form 27 January 2004; accepted 30 January 2004

Available online 22 April 2004

Abstract

The sulfurization behavior of $SrTiO_3$ nanoparticles was studied by using a quartz spring-type thermobalance in CS_2/N_2 atmosphere. The thermogravimetric curves showed the sulfurization of $SrTiO_3$ nanoparticles occurred at a temperature range from 150 to 750 °C accompanied with the maximum weight increase of 20.7%. A mixed sulfide as $Sr_{1.08}TiS_3$ was formed during the sulfurization process, and it showed sulfur loss at higher temperatures forming $Sr_{1.08}TiS_{3-x}$ as a final product at 1000 °C. In contrast, $SrTiO_3$ powders with larger particles size showed sulfurization at temperatures ranging from 550 to 950 °C forming $Sr_{1.08}TiS_3$, and no sulfur loss was observed at higher temperatures. The difference found in the sulfurization behavior was assigned to not only the particle size but also the presence of OH groups in the $SrTiO_3$ nanoparticles. During the sulfurization of calcined $SrTiO_3$ nanoparticles, the removal of OH groups of $SrTiO_3$ was found to produce an increment of the starting temperature of sulfurization.

Keywords: Strontium titanate; Thermogravimetry; Sulfurization; Strontium titanium sulfide; Carbon disulfide

1. Introduction

Strontium titanate ($SrTiO_3$) is well known as a functional material of excellent piezoelectric, ferroelectric, and dielectric properties and widely used for the production of gas sensors, transducers, non-volatile memories, capacitors, microwave devices, and insulating films. Furthermore, $SrTiO_3$ is a good catalyst for the CO_2 reforming or partial oxidation of methane owing to its stability at higher temperatures [1,2]. It is also appropriate for the photodecomposition of water [3,4].

On the other hand, metal sulfides have many interesting features such as electric and magnetic properties as well as high photoactivity under visible light, and in some cases they represent better performance than oxides. However, several metal sulfides are very sensitive to the oxidation in air or photodissolution in aqueous solution. In spite of this disadvantage, recently the sulfurization of oxides has received considerable attention because the sulfurized metal oxides have also shown higher optical, electrical, photoelectrochemical and photocatalytic activities than the non-sulfurized ones [5–10]. The partial sulfurization of $SrTiO_3$ powders is strongly expected as the same effect on the enhancement of their activities.

On the other hand, the particle size of oxides strongly affects their sulfurization behavior such as starting temperature of sulfurization [11,12], and only a partial replacement of oxygen in the structure by sulfur is necessary to produce noticeable changes in the oxide properties [8–10]. To obtain partially sulfurized $SrTiO_3$ powders with better photoactivity under visible light, the sulfurization behavior of $SrTiO_3$ nanoparticles is necessary to select an adequate temperature of partial sulfurization. In this regard, the thermogravimetric study of $SrTiO_3$ nanoparticles was carried out by using a quartz spring-type thermobalance in CS_2 atmosphere, and the results were compared with the sulfurization behavior of commercial $SrTiO_3$ powders with larger particle sizes.

2. Experimental

2.1. Materials

The $SrTiO_3$ nanoparticles were prepared according to the following procedure [13]. An amount of 0.05 mol of

* Corresponding author. Tel.: +81-22-217-5104; fax: +81-22-217-5104.
E-mail address: dragon@tagen.tohoku.ac.jp (N. Sato).

0040-6031/$ – see front matter © 2004 Elsevier B.V. All rights reserved.
doi:10.1016/j.tca.2004.01.033

tetraisopropyl orthotitanate (Tokyo Kasei Kogyo Co. Ltd.) was mixed with 0.1 mol of triethanolamine (Tokyo Kasei Kogyo Co. Ltd.) and this mixture was kept at room temperature in argon atmosphere overnight to form a stable Ti complex and to avoid uncontrollable hydrolysis. A stock solution was obtained by adding de-carbonated water to this mixture to make a total volume 100 ml. An amount of 0.2 mol of $Sr(OH)_2{\cdot}8H_2O$ (Wako Pure Chemical Ind. Ltd.) was dissolved in 10 ml of de-carbonated water. Then, 10 ml of the stock solution was added to this solution and stirred for 1 h. The resulting gel was heated in an autoclave at 250 °C for 3 h. Resultant solid was collected by centrifugal separation and washed with water under ultrasonication for three times. Finally, the nanoparticles were dried at room temperature for 24 h in air. For comparison, two commercial $SrTiO_3$ powders with larger sizes were also used as received; they were named STO-250 (99% purity, High Purity Chemicals Laboratory) and STO-450 (99.9% purity, Wako Pure Chemical Ind. Ltd.).

Analytical grade of CS_2 with a maximum water content of 0.02% (Wako Pure Chemical Ind. Ltd.) was used as received. Argon and nitrogen gases of 99.99% purity (Nippon Sanso Co. Ltd.) were used as received.

2.2. Thermogravimetric analysis

Thermogravimetric (TG) analyses of $SrTiO_3$ samples in Ar gas atmosphere were performed from room temperature to 1000 °C with a heating rate of 5 °C min^{-1} by using a Rigaku Thermoplus TG8120 analyzer. The gases liberated during the heating were analyzed by Shimadzu GC-MS QP5050 mass spectrometer.

In order to examine the sulfurization behavior, TG curves in CS_2 atmosphere were obtained by using a quartz spring-type thermobalance [11,12], which consists of a vertical resistance tube furnace and a quartz spring with a sensitivity of 6.70 mg mm^{-1}. A quartz crucible containing 300 mg of the sample was suspended from quartz spring at the center of the uniform temperature zone of the furnace. Before the measurement, the reaction tube was evacuated to ca. 100 Pa by a rotary pump for 30 min and then refilled with N_2 up to an ambient pressure. Then, CS_2 in N_2 carrier gas obtained by passing N_2 gas through a bubbler containing liquid CS_2 was introduced. The N_2 gas flow rate was measured using a digital mass flow meter (Kofloc Model DPM-2A). The sulfurization experiments were carried out at a heating rate of 1 °C min^{-1} from room temperature to 1000 °C with CS_2/N_2 flow rate of 5/50 ml min^{-1}. The change of the quartz spring length caused by the weight change was recorded by a levelmeter (Mitsutoyo) with an accuracy of 0.001 mm.

2.3. Characterization

X-ray diffraction patterns for the starting materials and their sulfurized products were obtained by using a Rigaku type RAD-IC diffractometer with a Ni filtered Cu Kα irradiation (40 kV and 20 mA) equipped with a curved pyrolitic carbon. The lattice parameters were calculated by using LCR2 program with silicon as a comparative standard [14]. Transmission electron microscope (TEM) images of the initial materials were taken using a JEOL JEM 2000EX electron microscope with an operating voltage of 200 kV.

3. Results and discussion

3.1. Characterization of initial materials

Fig. 1 shows the TEM micrographs of the starting materials. As show in Fig. 1(a), $SrTiO_3$ nanoparticles (STO-35) were found to be a well-crystallized cube of an average size of ca. 35 nm with a narrow size distribution. In contrast, commercial $SrTiO_3$ powders shown in Fig. 1(b) and (c) have average sizes of ca. 250 nm for STO-250 and 450 nm for STO-450. The morphology of these commercial $SrTiO_3$ powders was also cubic but agglomeration of the particles by sintering seemed to occur.

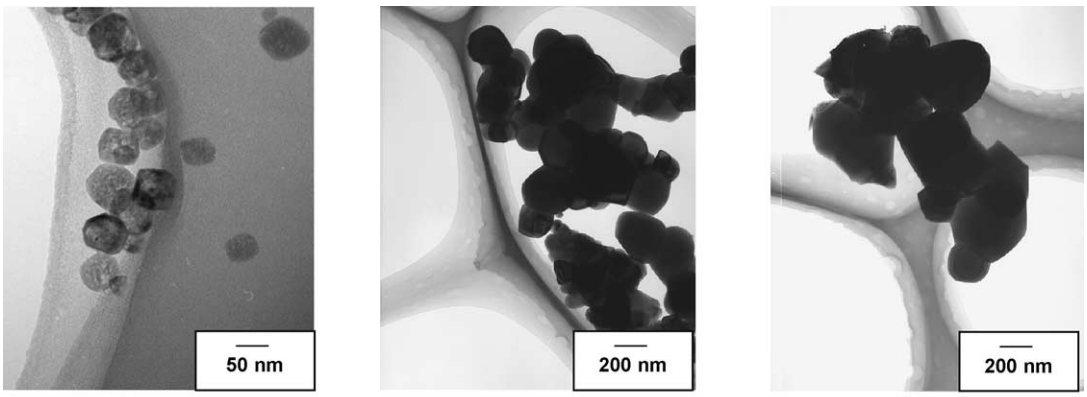

Fig. 1. Transmission electron micrographs of the $SrTiO_3$ samples as starting materials: (a) STO-35; (b) STO-250; (c) STO-450.

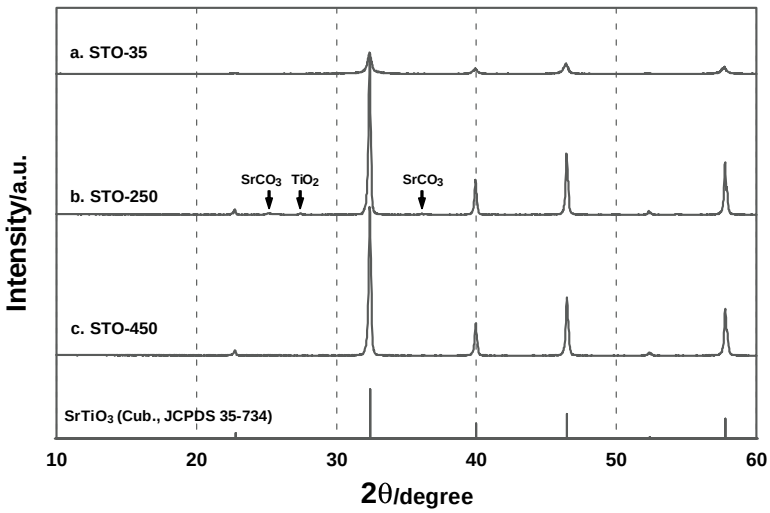

Fig. 2. XRD patterns of $SrTiO_3$ samples as starting materials.

The XRD patterns for these $SrTiO_3$ powders (Fig. 2) reveal that the three powders have mainly a cubic phase $SrTiO_3$ (JCPDS No 35-734), while $SrCO_3$ and TiO_2 (rutile) phases were found in STO-250 sample as impurities. The peaks of STO-35 broader than those of other two powders indicate the smaller size of STO-35 sample. An average size of 26 nm was calculated by the use of Scherrer's equation for the broad (1 1 0) peak of STO-35, which was slightly smaller than the results of TEM observation. This little difference between XRD and TEM in crystalline size means the mixture of single crystal with a little of polycrystals. In addition, by using step-scan XRD, the lattice parameter of STO-35 was calculated to be 0.3915 ± 0.0008 nm, slightly larger than the reported value (JCPDS No. 35-734), 0.3905 nm. This difference was attributed to the presence of OH groups in the structure of the oxide [15].

TG curves in argon atmosphere (Fig. 3) showed significant differences among these powders. TG curve of STO-35 (Fig. 3(a)) gave two steps. The first step is for the removal of adsorbed water occurred at temperatures below 160 °C with a weight loss of 4.0%, and the second one for dehydration occurred between 160 and 550 °C. Considering the weight losses by these two steps, the total amount of water content in the sample was estimated to be 6.7%. When the liberated gases during the heating were analyzed by GC-MS, only water was found but carbonate or organic compounds were not detected.

In the case of STO-250 (Fig. 3(b)), at temperatures lower than 500 °C, the sample did not show any weight change, but over 500 °C it revealed a weight loss of 0.9%, possibly because of the decomposition of carbonate such as $SrCO_3$ presented as an impurity. On the other hand, the TG curve of STO-450 sample (Fig. 3(c)) did not give considerable change in weight. As a result, water and/or hydroxide species were negligible for commercial $SrTiO_3$ samples, in contrast to $SrTiO_3$ nanoparticles (STO-35).

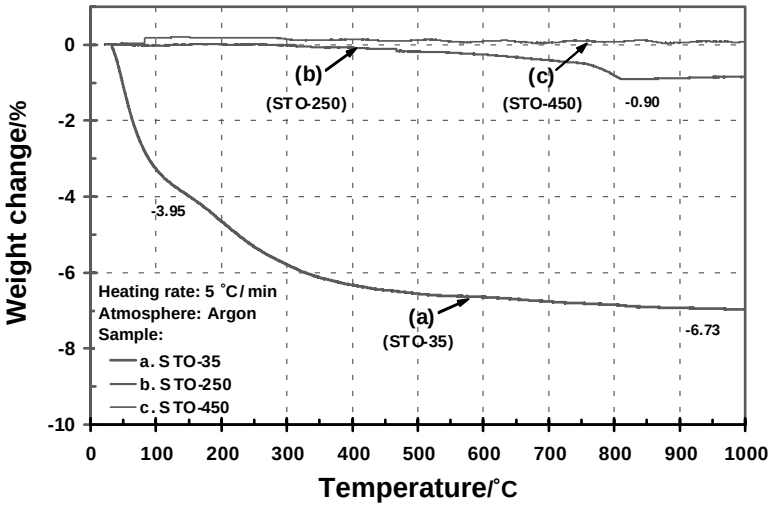

Fig. 3. Thermogravimetric curves of $SrTiO_3$ samples at a heating rate of 5 °C min^{-1} in Ar atmosphere.

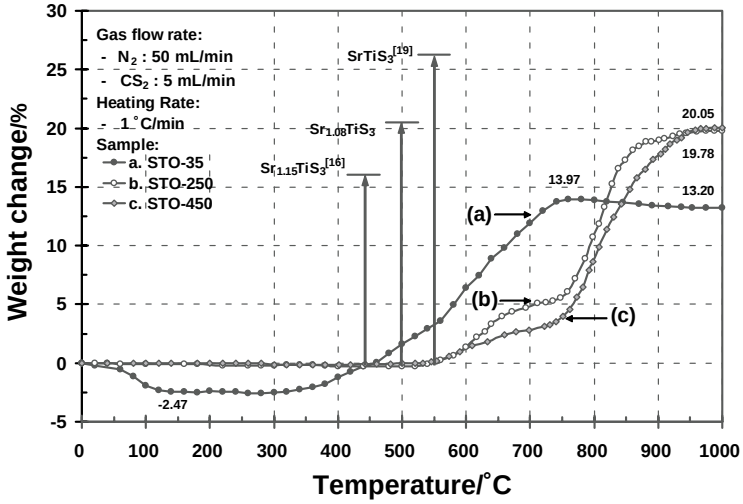

Fig. 4. Thermogravimetric curves of $SrTiO_3$ samples at a heating rate of 1 °C min^{-1} in CS_2/N_2 (5/50) atmosphere: (a) STO-35; (b) STO-250; (c) STO-450.

3.2. Sulfurization behavior of $SrTiO_3$ powders

TG curves for the reaction of the three $SrTiO_3$ samples with CS_2 are shown in Fig. 4. The theoretical weight increases for $Sr_{1.15}TiS_3$ [16] and $SrTiS_3$ [19] are also given for comparison. Apparently, the curve (a) for STO-35 sample is different from curves (b) and (c) for STO-250 and STO-450, respectively. For the latter, the TG curves (Fig. 4(b) and (c)) did not show any weight change at temperatures below 550 °C. Weight increase started at ca. 550 °C, and then two-step increase was found until 1000 °C. The first step from 550 to 750 °C may be caused by the partial replacement of oxygen by sulfur to form an intermediate phase like $SrTiO_xS_{1-x}$. The rapid increase in the second step indicated the complete sulfurization process of $SrTiO_3$. The sulfurization progressed until around 950 °C accompanied by a maximum weight gain of 19.8% for STO-250 and 20.1% for STO-450. Judging from pure $SrTiO_3$ for STO-450 (Fig. 3(c)), these findings suggest that $Sr_{1.08}TiS_3$ is obtained as a final product in both cases.

On the other hand, in the curve (a), initial decrease may be due to the removal of adsorbed water at temperatures below 140 °C with a weight loss of 2.5%. It seemed constant from 140 to 320 °C, clearly different from Fig. 3(a). Comparing the weight decrease of Fig. 3(a) and that of Fig. 4(a) at ca. 200 °C, the slight difference means the start of sulfurization of $SrTiO_3$ nanoparticles. With increase in temperature from 200 °C, the weight change was practically constant, in spite of the decrease in Fig. 3(a). The weight turned to increase after ca. 300 °C with increasing temperature and then reached to the maximum of 14.0% at ca. 750 °C. Judging from these facts, the starting temperature of the sulfurization must be ca. 150 °C. As mentioned in Section 3.1, the maximum weight decrease of $SrTiO_3$ nanoparticles (STO-35) was 6.7% in the heat treatment in Ar, i.e. in the absence of CS_2. Taking it into consideration, the maximum difference between decrease due to the removal of water and increase by the sulfurization was 20.7% (14.0 + 6.7), which was consistent with the values 19.8 and 20.1% for STO-250 and STO-450, respectively.

Fig. 5 shows the XRD patterns of the STO-35 samples obtained in temperature-programmed reaction with CS_2 from room temperature to 500, 550, 650, 750 and 1000 °C. Although the weight increase was found in the temperature range from 320 to 500 °C for the TG curve of STO-35 in Fig. 4(a), peaks corresponding to sulfides were not identified for the XRD pattern of 500 °C sample. Sulfide corresponding to $Sr_{1.15}TiS_3$ peaks appeared above 550 °C and the intensity of these peaks increased with increasing the temperature. In contrast to this, the peak height for $SrTiO_3$ decreased with increasing temperature and finally disappeared at 750 °C.

Since $Sr_{1.15}TiS_3$ is a refined form of Sr_yTiS_3 by using powder XRD data and y is ranged from 1.05 to 1.22 [16], the obtained $Sr_{1.08}TiS_3$ for TG (Fig. 4) is the same as $Sr_{1.15}TiS_3$ in XRD patterns (Fig. 5).

Figs. 6 and 7 show the XRD patterns of samples obtained by TG measurements of STO-250 and STO-450 with different final temperature at 500, 650, 750 and 1000 °C. Although the presence of impurity carbonate and titania was observed in ST0-250, there were no significant differences among these XRD patterns for sulfurized $SrTiO_3$ powders. XRD peaks of $Sr_{1.15}TiS_3$ appeared at temperature above 650 °C. In order to confirm the presence of intermediate phase the XRD pattern was taken for 650 and 750 °C samples. As is different from the XRD pattern of STO-35 (Fig. 5), $SrTiO_3$ phase still remained even at 750 °C for Figs. 6 and 7. The oxide peak shift to lower angles may be caused by the sulfur in the structure of oxide as well as the formation of an intermediate phase such as $SrTi_{3-x}S_x$. From TG curve, the probable amount of sulfur in the oxide varied approximately between 3.6 and 5.5%.

As shown in Fig. 4(a), the TG curve showed a considerable weight loss of 0.8% from 14.0 to 13.2% till 1000 °C. This was ascribed to the loss of sulfur from Sr_yTiS_3 (y =

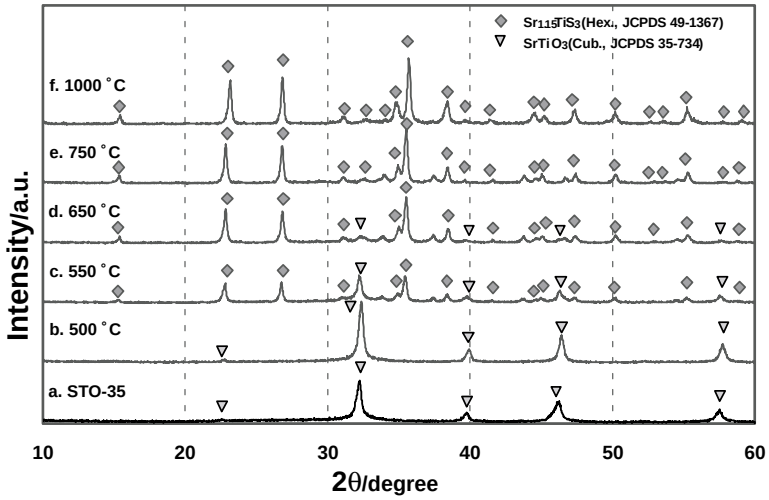

Fig. 5. XRD patterns of STO-35 obtained after the sulfurization at different temperatures.

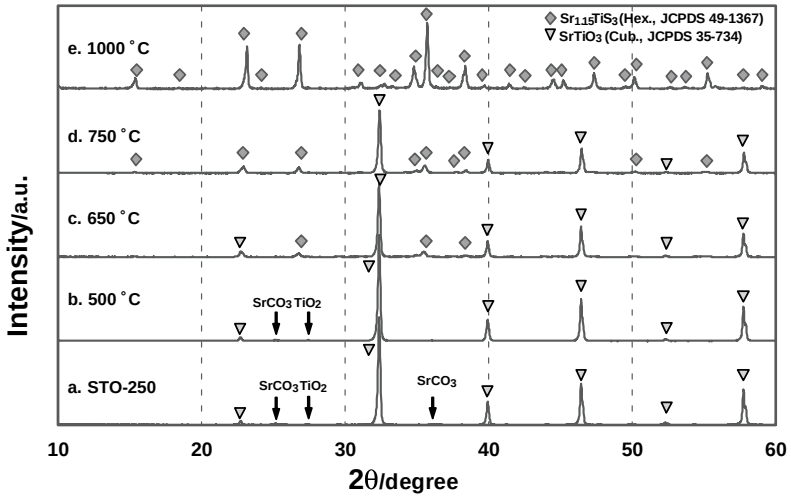

Fig. 6. XRD patterns of STO-250 obtained after the sulfurization at different temperatures.

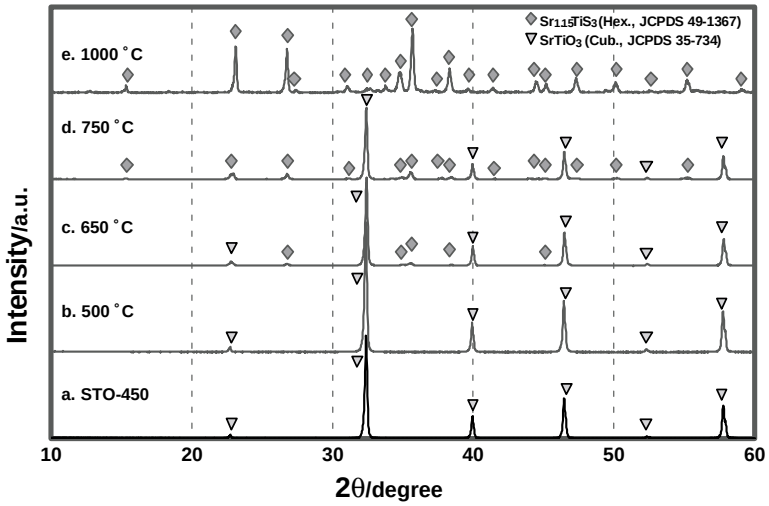

Fig. 7. XRD patterns of STO-450 obtained after the sulfurization at different temperatures.

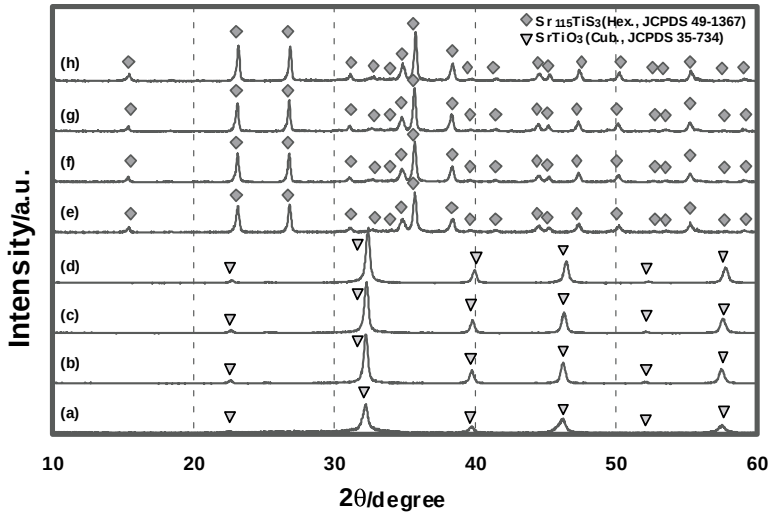

Fig. 8. XRD patterns of STO-35 samples calcined in air at different temperatures before sulfurization ((a) as-prepared, (b) 120 °C, (c) 250 °C, and (d) 500 °C), and after sulfurization ((e) as-prepared, (f) 120 °C, (g) 250 °C, and (h) 500 °C).

1.08 in this case) to the final product Sr_yTiS_{3-x} according to the results obtained by Saeki and co-workers [16–18]. However, the stoichiometric sulfide, $SrTiS_3$, described by Hahn and Mutschke [19] was not confirmed in our TG experiments.

3.3. Effect of calcination temperature

Since water or hydroxide group in $SrTiO_3$ nanoparticles (STO-35) can play a decisive role on the reduction in sulfurization temperature, the amount of OH groups was tried to decrease by the calcination. STO-35 sample was calcined in air at temperatures of 120, 250 and 500 °C for 5 h before the sulfurization. XRD patterns for those samples, Fig. 8(b)–(d), showed a better crystallinity than the starting material. By using the Scherrer's equation, the average particle size did not show any change for 120 and 250 °C calcined samples. However, an average particle size of 30 nm was found for 500 °C calcined one. On the other hand, the OH groups contained in the sample were difficult to be removed during the heating. A remaining amount of ca. 1.2% was found even at calcination temperature of 500 °C, calculated from weight decrease in heating it in Ar atmosphere from room temperature to 1000 °C.

Fig. 9 showed the sulfurization behavior of calcined $SrTiO_3$ samples. The TG curve for 120 °C calcined STO-35 (Fig. 9(b)) shows a starting temperature of sulfurization of 260 °C. The elimination of OH groups from its surface

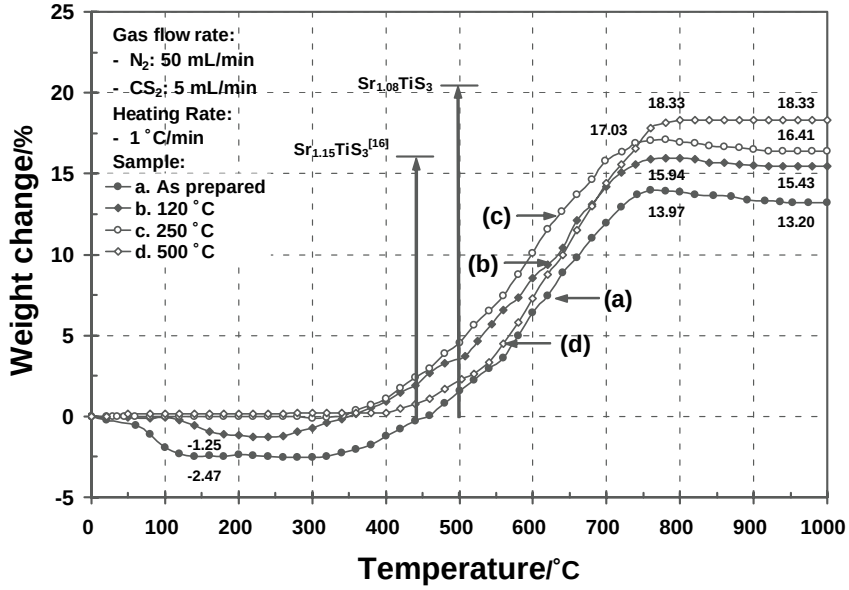

Fig. 9. Thermogravimetric curves of sulfurization of STO-35 samples calcined at different temperatures: (a) as-prepared; (b) 120 °C; (c) 250 °C; (d) 500 °C.

caused negative effects on starting temperature of sulfurization. Namely, it was increased to 340 for 250 °C-calcined STO-35 and 400 for 500 °C-calcined as seen in Fig. 9(c) and (d), respectively. It could be explained by the analogy of the report on the influence of water in the hydrolysis of CS_2 on TiO_2 [20], being carried out by means of a reaction between OH and CS_2. The maximum weight gain appears between 700 and 800 °C and Sr_yTiS_3 was formed.

Other researchers reported that the presence of surface defects favored the sulfurization on the surface [21,22]. In this case, the defects would be produced by removal of OH groups during the heating, becoming these sites very active to the sulfurization at low temperatures. On the other hand, oxygen would occupy those surface calcined of the material so that the starting temperature of sulfurization increased.

When the sulfurization of the 500 °C calcined sample was carried on up to 800 °C, the maximum weight increase of 18.3% was obtained. At higher temperatures it did not show any weight loss. The XRD patterns for as-prepared and the calcined STO-35 samples after the sulfurization until 800 °C (Fig. 8(e)–(h)) did not show any significant difference. Therefore, in accordance with TG curve, the final product described previously as Sr_yTiS_3 would be $Sr_{1.08}TiS_3$ similar to the sulfurized product obtained from commercial $SrTiO_3$ powders. However, the slight weight decrease, which may be caused by the loss of sulfur from the formed $Sr_{1.08}TiS_3$, was observed for 120 and 250 °C calcined samples.

4. Conclusion

In this study, thermogravimetric study of the sulfurization of $SrTiO_3$ nanoparticles using CS_2 was examined and the results are summarized as follows: Well-defined and homogeneous cubic $SrTiO_3$ nanoparticles were obtained from tetraisopropyl orthotitanate and strontium hydroxide as precursors. By TG using CS_2/N_2, not a stoichiometric sulfide, $SrTiS_3$, but a nonstoichiometric sulfide, $Sr_{1.08}TiS_3$, was obtained at 750 °C and it showed slight weight decrease by sulfur loss at 1000 °C. It was seen that the sulfurization of $SrTiO_3$ nanoparticles were favored by the reduction of particle size especially it reduced the starting temperature of sulfurization. However, the presence of OH groups also plays an important role in the reduction of the starting temperature of sulfurization. The sulfurization of $SrTiO_3$ nanoparticles seemed to proceed according to the next steps: (1) removal of adsorbed water; (2) adsorption of CS_2 and dehydration of OH groups; (3) formation of intermediate phase; (4) formation of sulfide.

Acknowledgements

One of the authors, J.C., thanks the Ministry of Education, Culture, Sports, Science and Technology of Japan, for financial support through the Monbukagakusho Scholarship. This work was partially supported by the Grant-in Aid for Scientific Research(s) No. 14103016 from the Ministry of Education, Culture, Sports, Science and Technology of Japan.

References

[1] T. Hayakawa, S. Suzuki, J. Nakamura, T. Uchijima, S. Hamakawa, T. Shishido, K. Takehira, Appl. Catal. 183 (1999) 273.
[2] K. Takehira, T. Shishido, M. Kondo, J. Catal. 207 (2002) 307.
[3] K. Domen, S. Naito, T. Onishi, K. Tamaru, Chem. Phys. Lett. 92 (1982) 433.
[4] F.T. Wagner, S. Ferrer, G.A. Somorjai, Surf. Sci. 101 (1980) 462.
[5] N. Sato, H. Masuda, M. Wakashima, K. Yamada, T. Fujino, J. Alloys Compd. 265 (1998) 115.
[6] P.M. Sirimanne, N. Sonoyama, T. Sakata, Chem. Phys. Lett. 350 (2001) 211.
[7] A. Di Paola, L. Palmisano, V. Augugliaro, Catal. Today 58 (2002) 141.
[8] R.J. Guo, M.H. Wang, T.L. Tso, T.P. Perng, Int. J. Hydrogen Energy 20 (1995) 561.
[9] M. Ziolek, J. Kujawa, O. Saur, J.C. Lavalley, J. Mol. Catal. A 97 (1995) 49.
[10] N. Sato, A. Muramatsu, K. Aoki, Y. Taga, Japanese Patent 074909 (2003).
[11] J. Cuya, N. Sato, K. Yamamoto, A. Muramatsu, K. Aoki, Y. Taga, Thermochim. Acta 410 (2004) 27.
[12] J. Cuya, N. Sato, K. Yamamoto, H. Takahashi, A. Muramatsu, High Temp. Mater. Proc. 22 (2003) 197.
[13] T. Sugimoto, Y. Masunaga, A. Muramatsu, in: Proceeding of the 52nd Symposium on Colloid Interface Chemistry, Morioka, 1999, p. 138.
[14] D.E. Williams, Ames Laboratory Report IS-1052, 1964.
[15] M.H. Frey, D.A. Payne, Phys. Rev. 54 (1996) 3158.
[16] M. Saeki, M. Onoda, J. Solid State Chem. 102 (1993) 100.
[17] M. Onoda, M. Saeki, A. Yamamoto, K. Kato, Acta Cryst. B 49 (1993) 929.
[18] M. Saeki, M. Ohta, K. Kurashima, M. Onoda, Mater. Res. Bull. 37 (2002) 1519.
[19] H. Hahn, U. Mutschke, Z. Anorg. Allg. Chem. 288 (1956) 269.
[20] H.M. Huisman, P. van der Berg, R. Mos, A.J. Van Pillen, J.W. Geus, App. Catal. A 115 (1994) 157.
[21] J.A. Rodriguez, J. Hrbek, Z. Chang, J. Dvorak, T. Jirsak, A. Maiti, Phys. Rev. B 65 (2002) 235414.
[22] E.L. Hebenstreit, W. Hebenstreit, H. Gaslev, C.S. Ventrice Jr., P.T. Springer, U. Diebold, Surf. Sci. 486 (2001) 467.